J. Phys. Earth, **23**, 257-278, 1975

TECTONIC IMPLICATIONS OF SUBCRUSTAL, NORMAL FAULTING EARTHQUAKES IN THE WESTERN SHIKOKU REGION, JAPAN

Kiyoji SHIONO* and Takeshi MIKUMO**

**Department of Geosciences, Faculty of Science, Osaka City University, Osaka, Japan*
***Disaster Prevention Research Institute, Kyoto University, Uji, Kyoto, Japan*

(Received March 12, 1975; Revised June 6, 1975)

Tectonic implications of subcrustal, normal faulting earthquakes in the western Shikoku region have been investigated in some detail, mainly based on the faulting mechanism of the Bungo channel earthquake of August 6, 1968 (M=6.6, h=45 km) and its aftershocks. A synthetic study of the focal mechanism solution, spatial distribution of aftershocks, seismic waves observed in the near and far fields, and vertical tectonic movements, indicates that the main shock was caused by normal faulting with some left-lateral motion of a western block downwards relative to the eastern side, along a steep westerly-dipping fault plane with dimension of 18–20 km, which was formed by the rupture initiating at a depth of 45 km and spreading upwards and northeastwards. The fault parameters estimated by a comparison between the observed and synthetic seismograms are: seismic moment 2.0–2.2$\times 10^{26}$ dyne·cm, average fault displacement 0.8–1.0 m and stress drop 33–40 bars. These parameters explain the measured elevation changes.

The focal mechanism of a series of the 1968 earthquakes, a foreshock, main shock and aftershocks, as well as many other earthquakes around the region, is consistently of the normal faulting type, in contrast to low-angled reverse faulting in Hyuganada earthquakes. This result suggests that all must have been generated under the same tensional stresses working horizontally in an E–W direction. Possible causes of the tensional stresses are discussed in relation to the descending Philippine Sea plate. Some tectonic models such as tearing, simple bending of the plate along the hinge line, gravitational drag, and thermal stress due to cooling, are tentatively examined.

1. *Introduction*

A relatively strong earthquake with a magnitude of 6.6 occurred on August 6, 1968, in the northeast part of the Bungo channel between the

Kyushu and Shikoku islands in southwest Japan (33°18.9′N, 132°23.3′E, h=45 km). The region including the Bungo channel and Iyonada, the west part of the Seto inland sea, is well known as a seismically active area; seven large earthquakes with magnitudes about 7 have occurred there repeatedly at an almost constant time interval of 40–60 years since 1600 (Fig. 1). The 1968 Bungo channel earthquake was the largest in magnitude since the Akinada earthquake of 1905. However, few detailed studies have been made so far as to seismic activity and source mechanism. ICHIKAWA (1971) has described some features of the focal mechanism of a number of subcrustal earthquakes during the period from 1926 to 1968, which include the present earthquake and some of its aftershocks. His results show that normal faulting earthquakes pre-

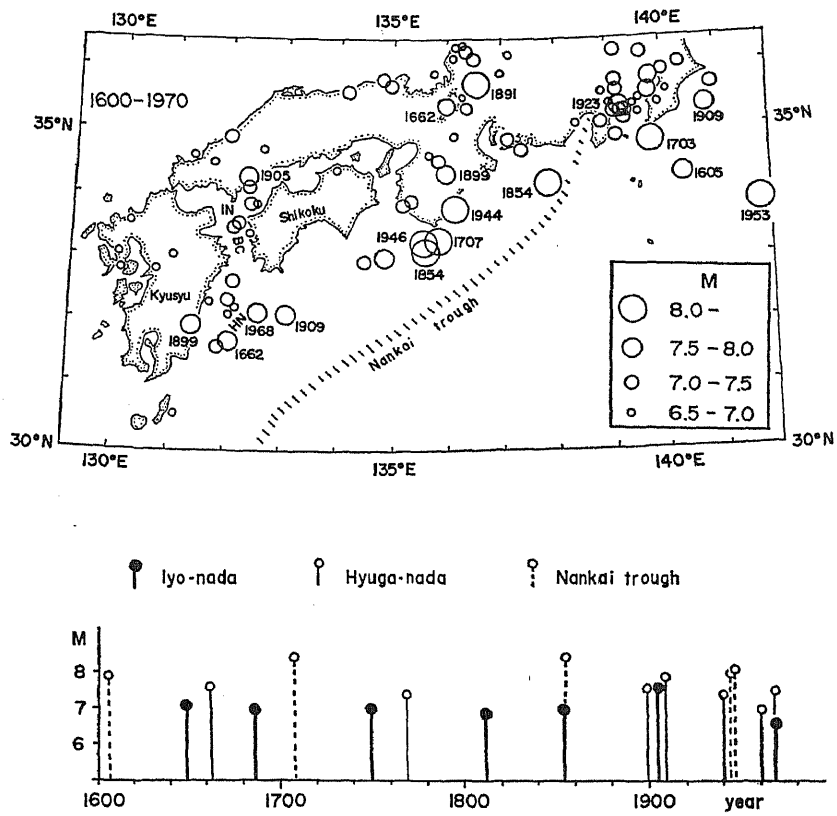

Fig. 1. Historical earthquakes in the period from 1600 to 1970, after USAMI (1966). Upper; epicentral distribution of earthquakes with magnitudes greater than 6.5. IN; Iyonada, BC; Bungo channel and HN; Hyuganada. Lower; time and magnitude for major earthquakes in the Bungo channel-Iyonada (closed circles and solid lines), Hyuganada (open circles and solid lines) regions and along the Nankai trough (open circles and broken lines).

dominate and that the axes of tension are more systematically oriented than the axes of compression, being nearly horizontally in the E–W direction. NISHIMURA (1973) also gave similar results for some of the earthquakes.

In sharp contrast to these earthquakes, great earthquakes such as the 1946 Nankaido and the 1968 Hyuganada earthquakes, which took place along the Nankai trough, are strongly characterized by thrust faulting on a very low-angled, northwestward dipping fault plane. Their mchanism have been interpreted as a result of elastic rebound on the interface between the continental Asian and the underthrusting oceanic Philippine Sea plates (FITCH and SCHOLZ, 1971; KANAMORI, 1972; ANDO, 1975). It has been revealed that the leading edge of the underthrusting plate reaches inland 150–200 km from the Nankai trough (KANAMORI, 1972; SHIONO, 1974; IKAMI and ITO, 1974). It is also noticed from Fig. 1B that there appear to be some periodicities and sometimes interrelationship between the occurrence of large earthquakes in the Hyuganada and the Bungo channel–Iyonada regions. These recent investigations appear to suggest that the normal faulting earthquakes in the Bungo channel–Iyonada region might have occurred in the zone of plate convergence, and that their mechanism might be closely associated with the shape and behavior of the descending oceanic plate. This possible relation in space and time greatly interested us.

The purpose of the present paper is to make clear the above possible relation or tectonic implications of the normal faulting earthquakes in this region on the basis of the faulting mechanism of the 1968 Bungo channel earthquake and the regional tectonic stresses inferred from fault plane solutions. The faulting mechanism is discussed in some detail from the spatial distribution of aftershocks, the radiation pattern of P-wave first motions, seismic waveforms and amplitudes in the near and far fields, and coseismic tectonic movements. A number of subcrustal earthquakes in southwest Japan are also examined.

2. *Re-determination of Hypocenters*

The Japan Meteorological Agency (JMA) has located 33 earthquakes that occurred around the source region of the 1968 earthquake during the period from January 1968 to December 1970. In the present study, for more precise location of the earthquakes, the hypocenters are re-determined using only P-wave arrival times obtained at six fixed stations, including five JMA stations, Uwajima (UWA), Matsuyama (MTY), Ashizuri (ASZ), Oita (OIT) and Hiroshima (HIR), and a microearthquake observation station Ugurusu (URS) operated by Kochi University (see Fig. 8). The least-square program used here is similar to that used conventionally in routine JMA work. Travel time

tables given by ICHIKAWA and MOCHIZUKI (1971) for an average crust-mantle structure are used here, though the velocity structure in the source region has not yet been surveyed. Because the Uwajima station provides data in a very near field ($\Delta = 10$–30 km), it is expected that these hypocenters can be deter-

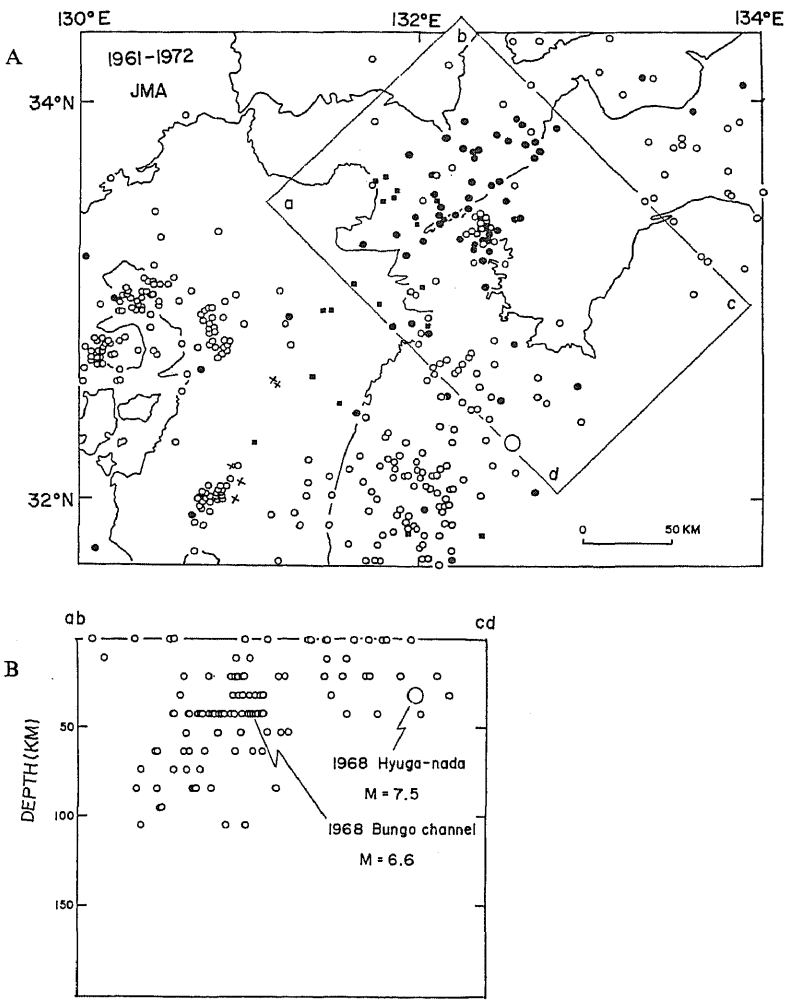

Fig. 2. Hypocentral distribution of earthquakes in the period from 1961 to 1972, based on the Monthly Seismological Bulletin of JMA. A: epicentral distribution. Different symbols indicate their focal depths; open circles, 0–30 km; solid circles, 40–70 km; solid squares, 80–110 km and cross marks, deeper than 120 km, respectively. B: vertical section. Hypocenters of earthquakes in a rectangle area abcd are projected onto a vertical plane ab–cd striking in the N45°W direction. A large circle shown in both A and B indicates the 1968 Hyuganada earthquake of magnitude 7.5.

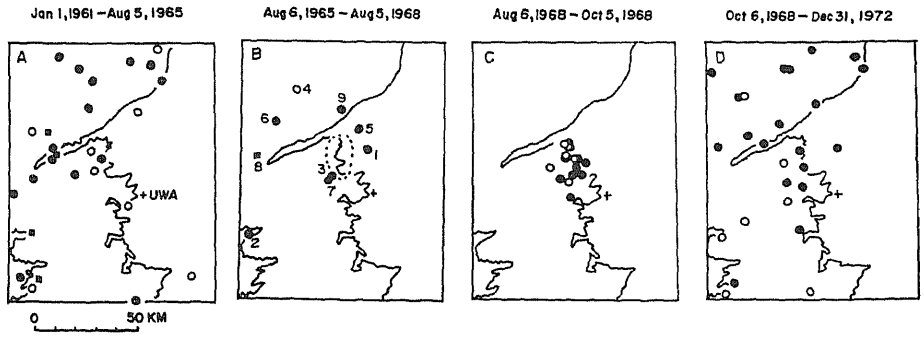

Fig. 3. Temporal variation of seismic activity near the source region of the 1968 Bungo channel earthquake. Different symbols indicate focal depths in the same manner as in the case of Fig. 2A. Location of the nearest station Uwajima is shown by a cross mark. In the period B, shocks of Nos. 1 and 2 occurred in 1966, Nos. 3 and 4 in 1967 and Nos. 5–9 in 1968, respectively. A shock of No. 5 is identical with that of No. 42 in Fig. 5. The source region of the 1968 earthquake is shown by a broken curve.

mined with relatively good accuracy. Judging from probable errors and a curve of focal depths vs. square sum of travel time residuals, the epicenters have been determined with a precision of 3 km and the accuracy of focal depths may be within 7.5 km. The hypocenters thus re-determined are shown in Fig. 5.

3. *Seismicity, Foreshocks and Aftershocks*

Based on the Monthly Seismological Bulletin of the JMA, epicentral distribution of earthquakes with magnitudes greater than 3 that occurred in the concerning region during the period from 1961 to 1972 is shown in Fig. 2A, with different symbols indicating their focal depths. It is shown that very shallow earthquakes are active in the Hyuganada region, while relatively deep shocks with depths ranging from 40 to 100 km are active in the Bungo channel–Iyonada region. For a better understanding of the seismic activity, shocks in a rectangle area abcd are projected onto a vertical plane striking in the N45°W direction, as shown in Fig. 2B. This figure shows a clear pattern of an active zone of earthquakes dipping northwestward at depths of 30–120 km.

Temporal variation of seismic activity during the period from 1961 to 1972 in the northern Bungo channel are shown in Fig. 3. The activity was relatively lower in 1966 and 1967, two years before the 1968 earthquake (Fig. 3B), compared with that in the periods 1961–1965 (Fig. 3A) and October 1968–1972 (Fig. 3D), but seems to become relatively high in 1968. The 1968 activity might be regarded as a foreshock activity. One of them was a relatively

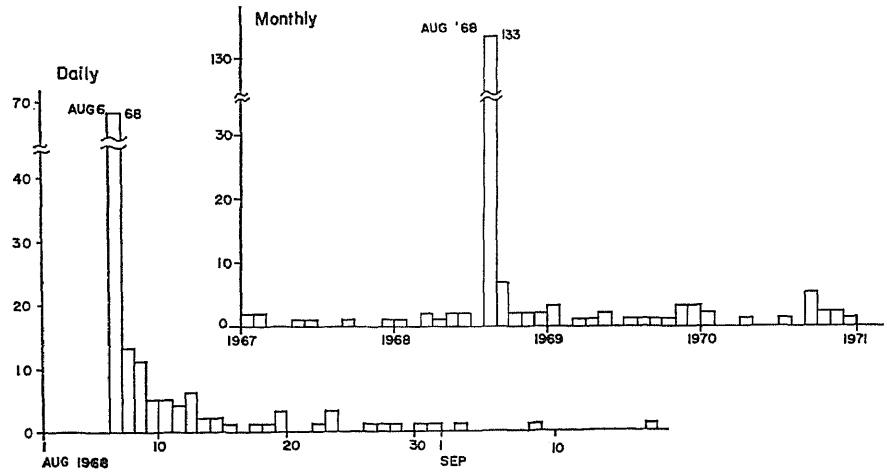

Fig. 4. Monthly and daily number of shocks with S–P time less than 6 sec recorded at a nearest station UWA.

large shock of magnitude 4.8, which occurred on January 1, 1968, about 50 km northeast. It is to be noted that these five foreshocks (Nos. 5–9) appear to have occurred so as to enclose the source region in a period shortly before the 1968 earthquake. Figure 4 shows the monthly and daily number of shocks with S–P times less than 6 sec recorded at the nearest station, Uwajima, indicating low seismicity in 1967. These evidence might be related to something like dilatancy hardening (SCHOLZ *et al.*, 1973). It is also interesting that no shocks were recorded within a month just before the main shock.

Following the main shock, 68 aftershocks were recorded at Uwajima within a day. Among them, there were three relatively large shocks (Nos. 50, 52 and 53, see Fig. 5) with magnitudes of 4.8, 4.9 and 5.3, respectively. The number of aftershocks decreased rapidly with time, and their major activity seems to have decayed within a few weeks as seen in Fig. 4, although a relatively high activity still remained for a few years (see Figs. 3 and 4). Thirty-one of these aftershocks re-located by the method described before are shown in Fig. 5. Different symbols indicate the periods of occurrence and magnitudes. Epicentral distribution of aftershocks within a month appears to be elongated in the NNE–SSW direction. Figure 5B shows the hypocenters projected onto two mutually perpendicular vertical sections, a–a′ striking in the N23°E direction and b–b′ in the N67°W, respectively. It can be seen from the former section that most of the aftershocks are distributed in an area with dimensions of 18–20 km by 18–20 km, and from the latter section that these aftershocks cluster around a steeply dipping plane. The main shock is located in the southwest and deeper portion of the aftershock zone (Fig. 5B).

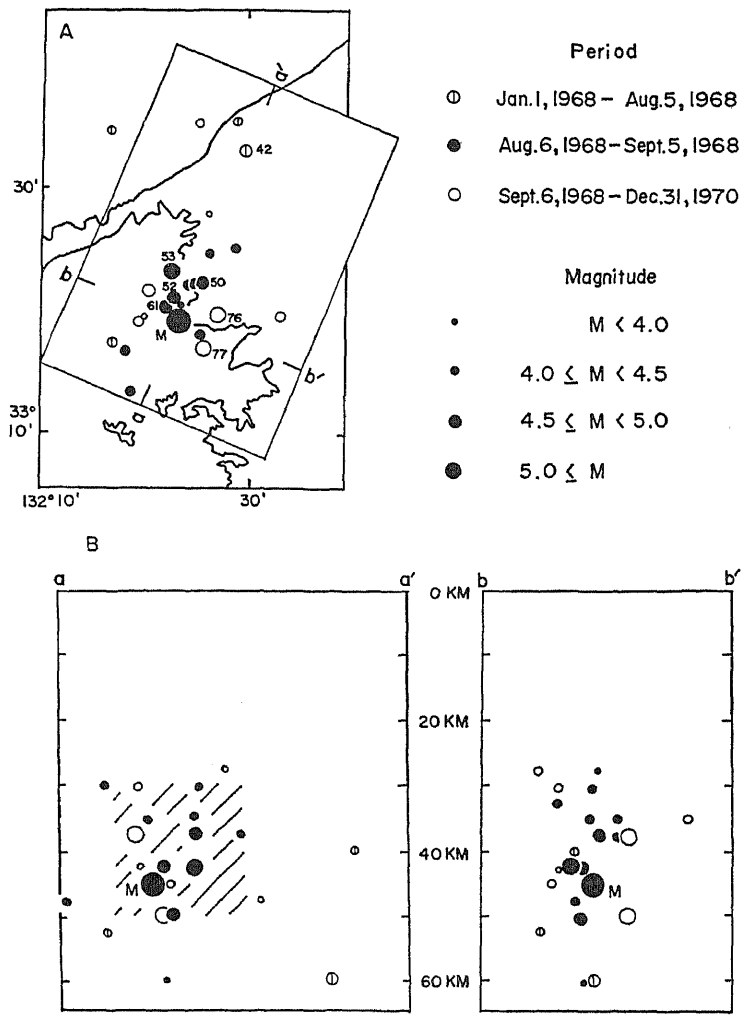

Fig. 5. Re-determined hypocenters of earthquakes in the source region in the period from 1968 to 1970. Different symbols indicate three periods as shown in the upper-right side. A large closed circle labeled as M give the hypocenter of the main shock. A: epicentral distribution. Numerals near epicenters give the index number in order to refer their fault plane solution shown in Fig. 7. B: vertical sections. Hypocenters of earthquakes in the area enclosed by a rectangle in Fig. 5A are projected onto two vertical planes a–a′ striking in the N23°W direction (left) and b–b′ in the N67°W direction (right), respectively.

4. *Fault-plane Solutions*

In the present study, focal mechanism of the main shock, foreshock and six aftershocks are precisely re-determined by incorporating various sources

of data. For the main shock, we use the P-wave first motions recorded on the vertical component of long-period seismograms at WWSSN stations, together with reports of JMA stations. In addition to JMA data, some supplementary data from university stations in southwest Japan are incorporated for a foreshock and aftershocks. To calculate the emergent angle of seismic rays leaving from the focus, an average crust-mantle structure of ICHIKAWA and MOCHIZUKI (1971) was used for Japanese stations at epicentral distances within 600 km, and the Jeffreys-Bullen velocity profile was applied to stations at teleseismic distances.

4.1 Main shock

The radiation pattern of P-waves from the main shock, including 126 data, is shown in Fig. 6, on the lower hemisphere of the Wulff net projection, where solid and open circles indicate compression and dilatation, respectively, and triangles correspond to nearby stations in the upper hemisphere. It can be noticed immediately that a nodal plane dipping towards N67°W with a dip of 72° is well defined, while the determination of another plane is somewhat uncertain within the range of two broken curves. Although we have two possible choices of fault plane from the two nodal planes, the radiation pattern clearly indicates normal faulting along either of the two planes as the mechanism of this earthquake. Since the trends of spatial distribution of aftershocks as shown in Figs. 5A and 5B seem generally consistent with the strike and dip of the first nodal plane, we may regard this plane as the fault plane of the main shock. No fault breaks were traced on the ground surface, presumably because the earthquake took place in the lower crust to uppermost mantle. The location of the main shock shown in Fig. 5B may be the initial point of

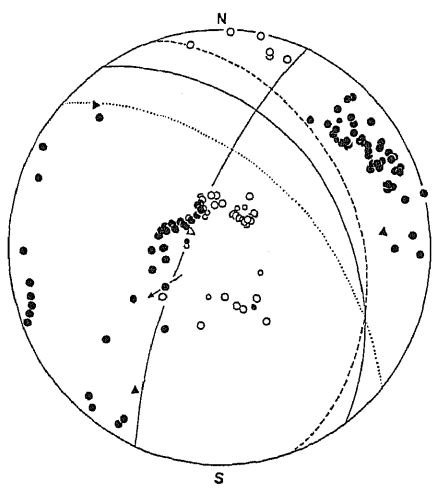

Fig. 6. Radiation pattern of P-wave first motions from the main shock, and its fault plane solution projected onto the lower hemisphere of the Wulff net. An arrow shows the direction of slip motion. Solid and open symbols indicate compression and dilatation, respectively. For other symbols, see text.

rupture. From these evidences, it may be reasonable to suppose that the main shock of the present earthquake was caused by normal faulting with some left-lateral motion of a western block downward against an eastern block along a steep westerly-dipping fault plane, which was formed by the rupture initiating at a depth of about 45 km and spreading almost bi-directionally upwards and northeastwards.

The faulting mechanism thus inferred may be modeled in such a way as schematically illustrated in Fig. 9. The fault plane dips towards N67°W by 72° with dimensions of 18–20 km by 18–20 km, on which point A is the location of the hypocenter, and B and C are the assumed alternative points of initial rupture. A thick arrow indicates the slip direction with a plunge of 148° and a trend of 235° for the motion of the western block, which can be estimated from the focal mechanism solution.

4.2 Foreshock and aftershocks

The focal mechanism of a foreshock (No. 42) and six major aftershocks (Nos. 51, 52, 53, 61, 76 and 77) has also been determined and is given in Fig. 7. It is remarkable that the foreshock with magnitude of 4.8 and most of the aftershocks are consistently of normal faulting type, similar to the case of the main shock; the strike and dip of one of their nodal planes are generally close to those of the main shock, and also seem parallel to the trend of aftershock distribution. The tensional axes of the above aftershocks and the foreshock are oriented nearly horizontally in the E–W direction, while the compres-

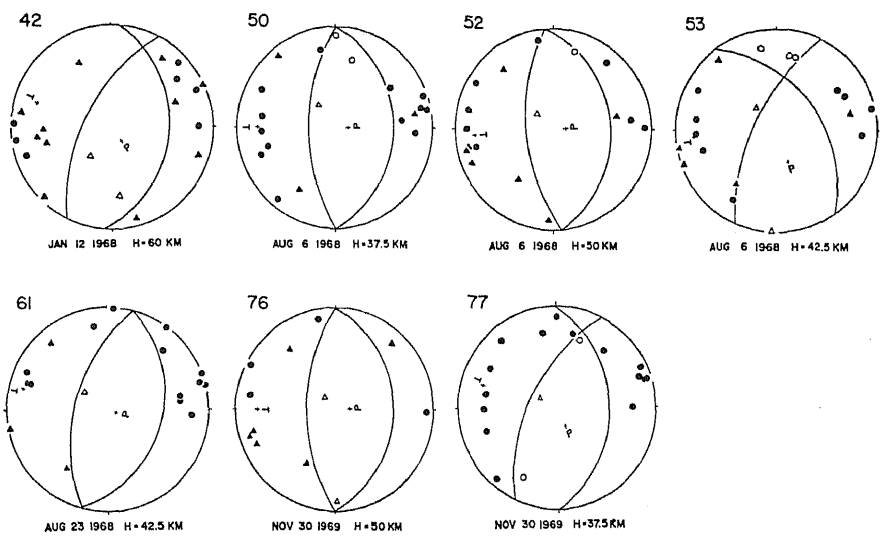

Fig. 7. Fault plane solutions of a series of the 1968 Bungo channel earthquakes. No. 42; a foreshock and Nos. 50, 52, 53, 61, 76 and 77; aftershocks.

sional axes dip steeply and are scattered over a rather wide range. This evidence suggests that the foreshock, main shock and aftershocks, all must have been generated under the same tensional stresses working over the region. This is also supported by the focal mechanism solutions of many other earthquakes that occurred around this region.

5. *Seismic Waves from the Main Shock*

5.1 Strong ground motion in the near field

During the present earthquake, strong ground motion with relatively long periods was recorded by conventional mechanical seismographs with a magnification nearly equal to 1 at seven JMA stations within 100 km from the epicenter. The largest ground amplitude recorded reached about 8 cm (peak to

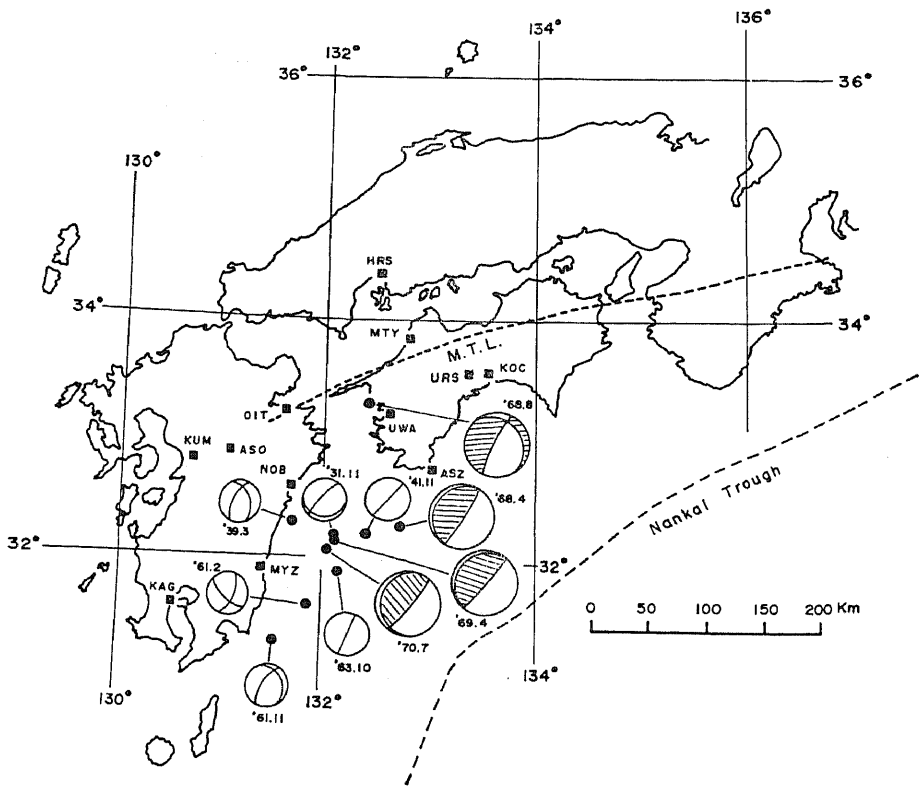

Fig. 8. Location of JMA stations (solid squares) equipped with strong motion seismographs, a micro-earthquake observation station URS, and fault plane solutions of earthquakes in the Bungo channel and Hyuganada regions. Large circles: fault-plane solutions of four recent earthquakes, in which hatched areas show compressional region.

peak) on the EW component at Uwajima, which is the most close-in station just east of the epicenter. The recorded seismogram is shown in the left-hand side of Fig. 10. Other recording stations are Matsuyama, Ashizuri and Kochi in the western Shikoku region, Oita and Nobeoka in the eastern side of Kyushu, and Hiroshima in southwestern Chugoku, which are indicated by solid squares in Fig. 8.

In order to clarify overall processes of dynamic faulting, we calculate theoretical ground displacements and synthetic seismograms in the near field from the assumed fault models, in comparison with the corresponding re-

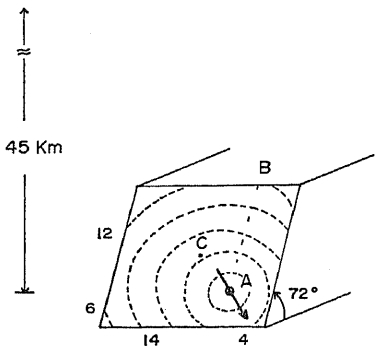

Fig. 9. Schematic illustration of the fault plane of the main shock. A: hypocenter. B and C: assumed alternative points of initial rupture. A thick arrow and broken curves indicate the slip direction of the upper block and wave front of rupture propagation.

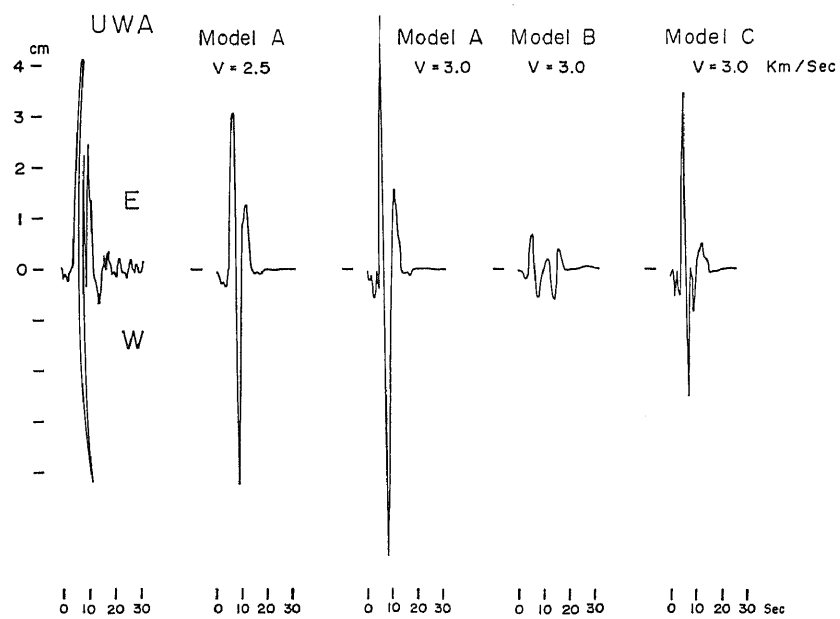

Fig. 10. Strong motion record (EW-component) observed at UWA (left end), and the corresponding synthetic seismograms with a rise time of 1 sec and rupture velocities of 2.5 and 3.0 km/sec. A, B and C are assumed initiating points of rupture.

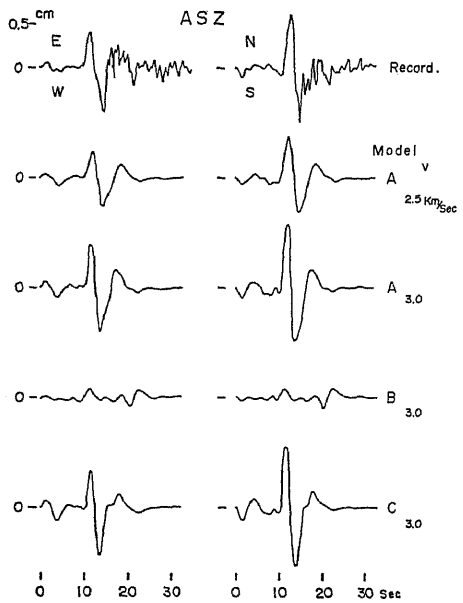

Fig. 11. Strong motion records observed at ASZ and the corresponding synthetic seismograms. For explanations, refer to Fig. 10.

cords. The method of calculation is based on the formulations given by MARUYAMA (1963) and HASKELL (1969) for dynamic dislocations in an infinite medium, with a simple correction to the free surface effects. In the above computation, we assume that the rupture initially started at the hypocenter A or alternative points B or C, and then propagated radially over the fault plane as schematically shown in Fig. 9, at velocities between 2.0 and 3.0 km/sec. As mentioned before, the crust-mantle structure in this region is not well known yet, we assume the average compressional and shear velocities to be 6.8 and 3.9 km/sec, respectively. The rise time of fault displacement τ is assumed to be 0.5–2.0 sec. Numerical calculations are made by a method similar to that described in MIKUMO (1973).

Figures 10 and 11 show the EW component record obtained at Uwajima (Δ=18 km) and two horizontal components of the records at Ashizuri (Δ=88 km), respectively, and the corresponding synthetic seismograms computed with two assumed rupture velocities and with a rise time of 1 sec. The comparisons among them, including all the computed seismograms not shown here, indicate that Model A (the rupture initiated at point A) with a rupture velocity between 2.5–3.0 km/sec appears to give the best agreement to the corresponding records at the two stations. In this case, allowance can be made for rise times between 0.5 and 1.5 sec. Case C also yields fairly good

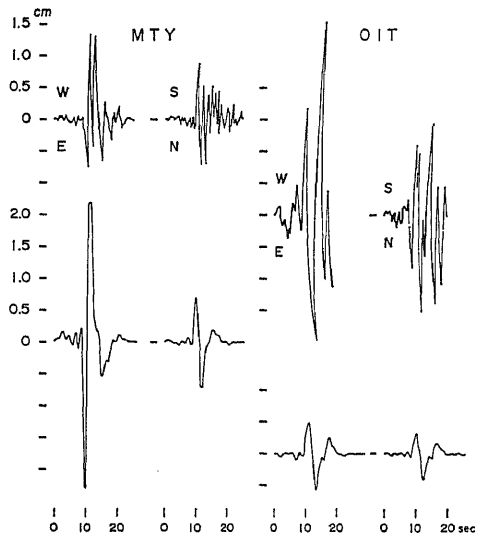

Fig. 12. Strong motion records observed at MTY and OIT, and the synthetic seismograms for Model A with $\tau=1$ sec and $v=2.5$ km/sec.

approximations and hence cannot be rejected. It is evident, however, that the agreement reduce to be only poor, if the rupture were propagated downwards from point B at the upper rim of the fault plane. These situations suggest that the rupture was actually initiated around the hypocenter A and then spread upwards and northeastwards. Figure 12 also gives comparisons between the observed and synthetic seismograms with a rupture velocity of 2.5 km/sec at Matsuyama and Oita. It is noticed that discrepancies in the absolute amplitudes are rather serious at Oita, although their waveforms up to about 12 sec are somewhat similar. This is also the case for the Nobeoka station in eastern Kyushu. These discrepancies might be attributed to some amplification effects due to surficial and upper crustal structures, since they cannot be reconciled by changing the various fault parameters in a reasonable range.

5.2 Far-field observations

Direct P and S waves from the main shock have been clearly recorded on the long-period seismograms at a number of WWSSN stations. Some examples of the vertical component seismograms are shown by solid curves in Fig. 13. It is noticed that later phases, such as pP, sS and sometimes sP which are reflected at the ground surface near the source, arrive 12–25 sec later with appreciable amplitudes, but do not seem to contaminate the waveforms of the first half to one cycle of the direct waves. To obtain additional information on the focal process, we compute synthetic seismograms of direct body waves

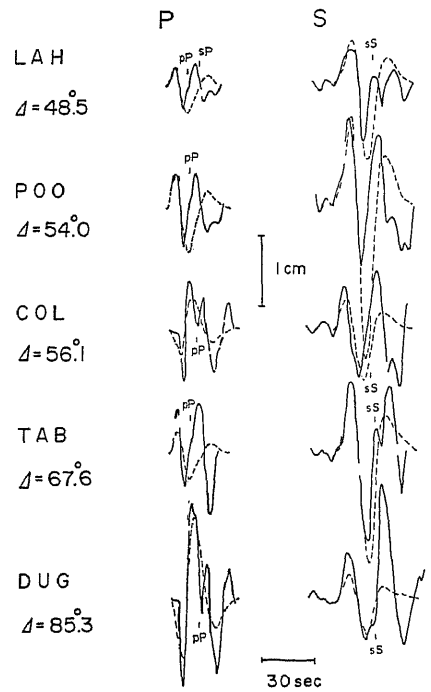

Fig. 13. Long-period seismograms (vertical component) recorded at WWSSN stations in teleseismic distances (solid curves) and the synthetic seismograms (broken curves).

for 12 stations at teleseismic distances from the fault model described before, and compare them with the above records. The method is essentially the same as that has been applied to the case of intermediate and deep focus earthquakes (MIKUMO, 1971), which includes the effects of the source, divergence and attenuation along the wave path, crustal structure under recording stations and of seismograph response. The computed seismograms are given by broken curves in Fig. 13. Since the above computations do not include surface-reflected later phases, comparison with the observed records has to be limited to the first half to, at most, one cycle. For the limited time interval, agreement in the waveforms and amplitudes between the observed and computed traces appears generally satisfactory except for slightly shorter periods of the observed P waves at COL and DUG.

The observed and computed amplitudes are directly compared in Fig. 14, where the maximum double amplitudes (corresponding to S waves in most cases) are taken in the case of near-field observations (solid circles), and the amplitudes of the first half cycle are plotted for both P (open circles) and S (triangles) waves in the case of teleseismic observations. Although deviation

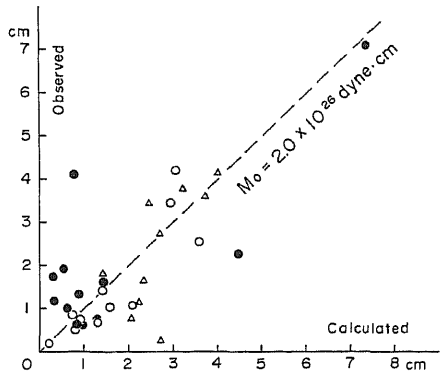

Fig. 14. Observed and calculated wave amplitudes. Solid circles; maximum double amplitudes for near-field stations. Open circles and triangles correspond to the amplitudes of first half-cycle of P and S waves at teleseismic distances.

from a mean straight line is significant for a few points, this comparison yields the average seismic moment of $2.0\text{–}2.2 \times 10^{26}$ dyne·cm. Combining the moment and the fault dimension which has been estimated from the extent of aftershock distribution, the average fault displacement and the stress drop are estimated to be about 0.8–1.0 m and 33–40 bars, respectively, if the crustal rigidity is taken as 6×10^{11} dyne/cm^2.

6. *Tectonic Movements*

To estimate tectonic surface movements due to deep faulting in the present earthquake, and to compare them with the elevation changes derived from leveling surveys, theoretical displacements are computed from the assumed model, referring to the formulations given by MARUYAMA (1964) for static dislocations in a half-space. The fault parameters such as the orientation, dimension and displacement (1 m) are taken to be the same as in the foregoing model. Figure 15 illustrates the pattern of the computed vertical movements, which are represented by contour lines of subsidence (broken curves) and uplift (solid curves). The rectangle enclosed by fine broken lines and a thick arrow indicate the horizontal projection of the assumed fault plane and the slip direction of a western block, respectively. It is found that the expected maximum subsidence exceeds 3 cm, which is large enough to be detected by precise leveling surveys.

The leveling surveys in this region were made by the Geographical Survey Institute in June–December, 1964, four years before the 1968 earthquake, and again in May–December, 1971, three years after the earthquake, along a route through Uchiko (B.M. 4555), Yawatahama (B.M. 4569), Uwajima

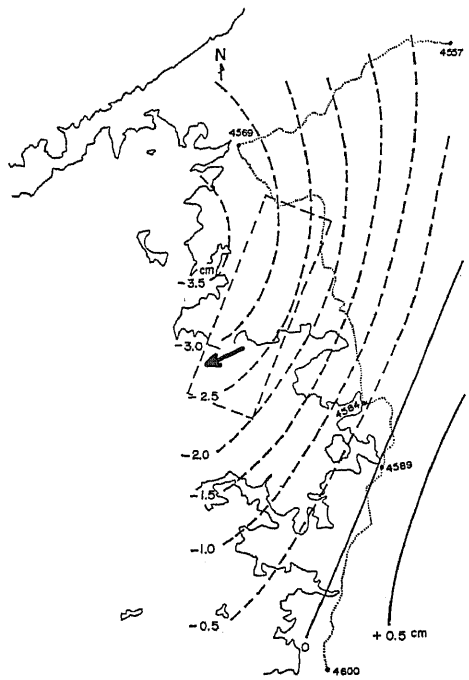

Fig. 15. Pattern of the vertical, static displacements computed from the assumed fault model. Thick and broken curves indicate uplift and subsidence, respectively. Rectangle, horizontal projection of the fault plane, thick arrow, slip direction of the western block and fine dotted line, leveling route.

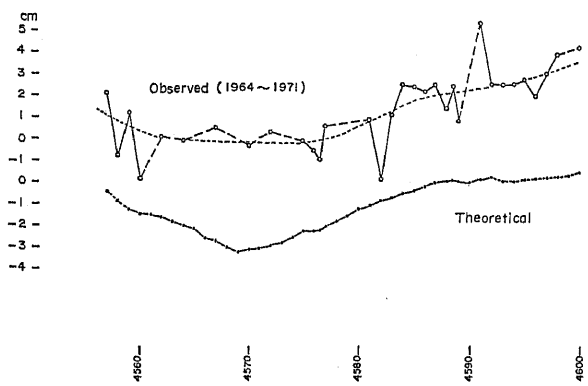

Fig. 16. Vertical tectonic movements (1964–1971) along the leveling route and the corresponding vertical displacements computed from the fault model.

(B.M. 4589) to Tsushima (B.M. 4600). The route is shown by a fine dotted line in Fig. 15. The level changes derived from the two surveys (GEOGRAPHICAL SURVEY INST., 1972) are reproduced in the upper part of Fig. 16, in

comparison with the vertical displacements computed from the fault model. It is probable that the measured changes might not exactly represent the tectonic movements due to the 1968 earthquake, since there could be pre- and post-seimic movements as suggested by FUJITA and FUJII (1973) between the above two periods. Nevertheless, we notice that the general trend of the changes indicated by a broken curve almost run parallel to that of the theoretical displacements with a small difference of about 3 cm over the entire route. This difference in the absolute amplitude is not essential, because the level of the measured changes has been adjusted to be zero at a point on the route. Thus, it may be concluded that most part of the level changes can be interpreted as co-seismic movements, or at least, are not inconsistent with the fault motion inferred from seismic wave observations.

7. *Discussion*

7.1 Possibility of another faulting mechanism

Various evidence given in the foregoing sections appears to support the interpretation that the main shock of the 1968 earthquake was caused by normal faulting of the western block that slipped down relative to the eastern side along a steep westerly-dipping fault plane under tensional stresses working nearly horizontally in an E–W direction. However, the present model is subject to the criticism on the determination of the fault plane because the spatial distribution of aftershocks is not so clearly delineated and the larger seismic wave amplitudes are recorded in eastern Kyushu. We shall discuss here the possibility of faulting along another nodal plane dipping towards the northeast: this model is called here an alternative model.

If the aftershocks are projected on a vertical section perpendicular to the alternatively assumed fault plane, their distribution becomes less concentrated, compared with that in the former model. Static and dynamic ground displacements are again computed on the basis of the alternative model. The seismic moment is taken to be the same as that estimated before because there was general agreement between the observed and theoretical amplitudes of the far-field seismograms. The computed static ground displacements show a somewhat different pattern with a more gentle tilt towards the NE direction. Theoretical subsidence reduces to about 2 cm at maximum, and its trend along the leveling route yields a slight deviation towards south from measured level chages. However, this cannot be conclusive evidence to discriminate the fault plane. The large discrepancies on the dynamic displacements at the two stations on the eastern side of Kyushu are only slightly improved. A decrease in the computed amplitudes is somewhat noticeable for the Matsuyama station, but not for the other stations. A most serious discrepancy comes out,

however, from the alternative model; the theoretical amplitude of the EW component at Uwajima reduces down to 3.5 cm in contrast to the recorded amplitude of 8 cm, whereas the former model has yielded a good agreement. We think that this last evidence favors the first interpretation, since the Uwajima station is almost right above the fault plane. This interpretation seems generally consistent with tectonic features that the trend of the coastal line in northwestern Shikoku runs nearly in the N–S direction and also with geomorphological evidence of the coast descending towards the Bungo channel.

The estimated fault parameters for the first model are summarized in Table 1.

Table 1. Fault parameters of the main shock.

Dip	72°
Dip direction	293°
Slip direction	235°
Fault length	18–20 km
Fault width	18–20 km
Seismic moment	$2.0–2.2\times10^{26}$ dyne·cm
Average displacement	0.8–1.0 m
Fracture velocity	2.5–3.0 km/sec
Rise time	0.5–1.5 sec
Stress drop	33–40 bars

7.2 Focal mechanism of subcrustal earthquakes in southwest Japan

Seismic activity at depths 30–80 km can be traced throughout the Outer Zone of southwest Japan from the Iyonada–Bungo channel region, Shikoku Island, Kii peninsula to the southern Chubu regions (SHIONO, 1974), from observational surveys of microearthquakes as well as from the hypocentral distribution of subcrustal earthquakes determined by the JMA. A number of studies on the focal mechanism of these earthquakes have been made so far. The mechanism of earthquakes in the Iyonada region generally shows normal faulting with tensional stresses working horizontally in an E–W direction (ICHIKAWA, 1971; NISHIMURA, 1973). In the Kii peninsula region, the 1952 Yoshino ($H=70$ km, $M=7.0$), the 1960 Odaigahara ($H=60$ km, $M=6.0$) and two 1973 west Kii peninsula ($H=50$ km, $M=6.0$) earthquakes were large earthquakes in the uppermost mantle and have tensional axes oriented horizontally in a NE–SW direction, although the 1952 and 1960 shocks show strike-slip faulting and the 1973 shocks show nearly pure normal faulting (M. Nakamura, personal communication, 1974). For smaller earthquakes in the same region, the tensional axes are also oriented in the above direction in spite of a variety of faulting type (ICHIKAWA, 1971; SHIONO, 1973). In the southern Chubu region, the tensional axes of small shocks at depths

below 25 km are also oriented horizontally in an E–W direction, while the pressure axes vary rather randomly (OOIDA and ITO, 1974). The above evidence seems to suggest that the subcrustal earthquakes are generated by tensional stresses working over the entire region in an E–W or NE–SW direction; this direction is perpendicular to the descending direction of the Philippine Sea plate (SHIONO, in preparation, 1975). It might be possible to consider from the above discussions that the 1968 Bungo channel earthquake is caused by prevailing stress rather than by local stresses acting exceptionally in the source region.

7.3 Tectonic implications

We shall discuss here some possible causes of the normal faulting earthquakes in the region now considered, in view of subduction of the Philippine Sea plate. SHIONO (1974) has presented a probable, tectonic model for the spatial extent of the Philippine Sea plate descending underneath southwest Japan along the Nankai trough (see Fig. 15 in his paper), on the basis of travel time analysis and seismic activity of subcrustal earthquakes. His result shows that the leading edge of the descending plate reaches a line going through central Kyushu to Iyonada–northern Shikoku and crosses obliquely the Kii peninsula and extending east to north Izu peninsula. The depth of the edge seems to extend down to about 100 km beneath Kyushu and to become shallower to about 40–50 km towards east side.

7.3.1 Coupling mechanism

The subduction of the Philippine Sea plate from the Nankai trough is more extensive and also deeper towards Kyushu than towards Shikoku–Kii. This situation suggests that there could be bending or contortion of the plate under a line through the Iyonada–Bungo channel. It is possible to suppose qualitatively that these circumstances would yield stresses to drag the descending oceanic plate down and westwards by gravitational pull. The simplest idea is to assume that the above drag force would produce tearing or disruption of the plate along the above line, as suggested by ISACKS and MOLNAR (1971) for mantle earthquakes beneath central Honshu; faulting motion would be nearly vertical, in such a way that the more steeply dipping west-side moves down relative to the more gently dipping east-side. This mechanism of hinge faulting would appear to account for some features of the 1968 earthquake. However, the following evidence is inconsistent with this interpretation; the P-wave arrivals of the present earthquake and its aftershocks show a high apparent velocity of about 9 km/sec, being followed by a later phase with a normal velocity of 8 km/sec arriving 0.5–1.0 sec later in the southern Shikoku region (SHIONO, 1974). In view of the short time interval between the first and later phases, a likely explanation is that the first P-waves are refracted at

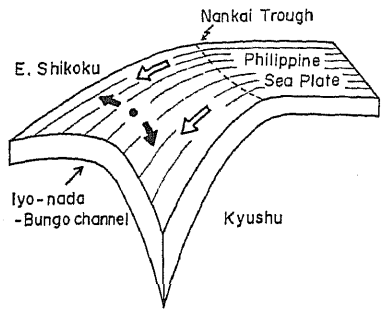

Fig. 17. A possible tectonic model which could explain normal faulting earthquakes due to horizontal tensional stress (thick arrows).

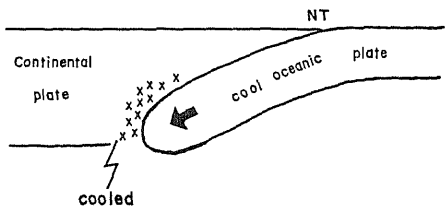

Fig. 18. Another possible model which could explain normal faulting earthquakes.

a high velocity layer of an oceanic plate and the later phase may be direct P-waves transmitted through a normal mantle (SHIONO, 1974). This explanation implies that the 1968 earthquake has occurred probably just above the interface between the continental and oceanic plates.

The above situation suggests that the present earthquake is not caused by disruption of the plate itself or rebound of continental lithosphere as in Hyuganada earthquakes. It may be reasonable to consider that the earthquake is caused by internal deformation of the bottom of the continental lithosphere, due to simple bending of the oceanic plate or gravitational drag of the plate down- and northwestwards. The bending would be able to yield tensional stresses oriented in the E–W direction just above the plate, along the axis of bending through the Bungo channel–Iyonada. Although the deformed effects should be locally confined there, this explanation seems quite plausible. This model is schematically illustrated in Fig. 17. Tensional stresses might also be produced from the gravitational drag in and above the oceanic plate over wide regions, if the eastern side of the plate is fixed to some point. Actually, the Philippine Sea plate appears to be depressed to the continental lithosphere at the northern part of the Izu peninsula, due to its northwestward movement. This interpretation also seems possible.

7.3.2 Thermal mechanism

As the leading edge of the sinking oceanic plate penetrates into the continental plate and moreover only a million years at most have passed since the oceanic plate began to underthrust (e.g., FITCH and SCHOLZ, 1971), it might be possible that the temperature is decreasing rapidly in the continental plate near the interface due to the penetration of the cool oceanic plate. Thermal stresses would be generated along the margin of the continental plate due to such a change of temperature. If the upper surface of the continental

plate and the interface between the two plates are assumed to be free surfaces, the vertical component of the stresses and the component normal to the trench axis would be released by contraction of the continental plate. As a result, only a component parallel to the trench axis would really act in the continental margin, as shown in Fig. 18. Thermal stresses σ due to cooling may be simply estimated by $\sigma \sim \alpha ET$, where α, E and T are coefficient of volumetric thermal expansion, Young's modulus and temperature difference, respectively. If the values of these parameters are taken to be $\alpha = 4 \times 10^{-5} °C^{-1}$ (SKINNER, 1966), $E = 10^{12}$ dyne $\cdot$ cm^{-2} and 100°C, $\sigma \sim 4$ kbars. Since this simple calculation shows that tensional stresses due to cooling are large enough to generate earthquakes, such thermal stresses would play a fundamental role of the generation of normal faulting earthquakes at the continental plate margin, which is subjected to hydrostatic pressures of the orders of 10 kbars. This speculation could explain the feature that the tensional axes of subcrustal earthquakes in southwest Japan are generally oriented in the E–W direction in spite of a variety of the pressure axes.

In view of the lack of uniqueness, the choice of a reasonable model is now difficult and must await further study. The key is the study of mechanism as well as seismicity of a number of subcrustal earthquakes in southwest Japan.

We wish to thank Dr. Masataka Ando and Mr. Koichi Nakagawa for discussion on the present study, and Mr. Masao Nakamura for his unpublished results. We are also grateful to Dr. Mamoru Katsumata of the Japan Meteorological Agency for supplying us copies of strong-motion records, Mr. Shozo Kimura of Kochi University for observed data, and to Dr. Hiroshi Sato of the Geographical Survey Institute of Japan for providing the leveling data. Copies of the WWSSN seismograms were provided by the NOOA, U.S.A. Our thanks are extended to Mrs. Ritsuko Koizumi and Mr. Yoshinobu Hoso for their assistance in the present work.

The computations involved were made at the Data Processing Center of Kyoto University and also at the Computer Center of Osaka City University.

REFERENCES

ANDO, M., Source mechanisms and tectonic significance of historical earthquakes along the Nankai trough, Japan, *Tectonophysics*, **27**, 119–140, 1975.

FITCH, T. J. and C. H. SCHOLZ, Mechanism of underthrusting in southwest Japan: A model of convergent plate interactions, *J. Geophys. Res.*, **76**, 7260–7292, 1971.

FUJITA, N. and Y. FUJII, Detailed phases of seismic crustal movement, *J. Geod. Soc. Japan*, **19**, 55–56, 1973.

GEOGRAPHICAL SURVEY INSTITUTE, *Results of first-class leveling surveys*, **16**, 1972 (in Japanese).

HASKELL, N. A., Elastic displacements in the near-field of a propagating fault, *Bull. Seism. Soc. Amer.*, **59**, 865–908, 1969.

ICHIKAWA, M., Reanalyses of mechanism of earthquakes which occurred in and near Japan, and statistical studies on the nodal plane solutions obtained, 1926–1968, *Geophys. Mag.*,

35, 207–274, 1971.

ICHIKAWA, M. and E. MOCHIZUKI, Travel time tables for local earthquakes, *Pap. Met. Geophys.*, **22**, 229–290, 1971 (in Japanese).

IKAMI, A. and K. ITO, Seismic waves traveling from southwest Japan to Inuyama Seismological Observatory—Existence of a high-Q zone in southwest Japan, *Zisin*, **27**, 225–238, 1974 (in Japanese).

ISACKS, B. and P. MOLNAR, Distribution of stresses in the descending lithosphere from a global survey of focal-mechanism solutions of mantle earthquakes, *Rev. Geophys. Space Phys.*, **9**, 103–174, 1971.

KANAMORI, H., Tectonic implication of the 1944 Tonankai and the 1946 Nankaido earthquakes, *Phys. Earth Planet. Interiors*, **5**, 129–139, 1972.

MARUYAMA, T., On the force equivalents of dynamical elastic dislocations with reference to the earthquake mechanism, *Bull. Earthq. Res. Inst.*, **41**, 467–486, 1963.

MARUYAMA, T., Statical elastic dislocation in an infinite and semi-infinite medium, *Bull. Earthq. Res. Inst.*, **42**, 289–368, 1964.

MIKUMO, T., Source process of deep and intermediate earthquakes as inferred from long-period P and S waveforms, 1 and 2, *J. Phys. Earth*, **19**, 1–19, 1971; **19**, 303–320, 1971.

MIKUMO, T., Faulting process of the San Fernando earthquake of February 9, 1971 inferred from static and dynamic near-field displacements, *Bull. Seism. Soc. Amer.*, **63**, 249–269, 1973.

NISHIMURA, K., Characteristic features of focal mechanism in and near Kyushu island (1), *Contr. Geophys. Inst., Kyoto Univ.*, **13**, 101–110, 1973.

OOIDA, T. and K. ITO, Focal mechanism of shallow earthquakes which occurred in the east part of Kinki district and Chubu district, central Honshu, Japan, *Zisin, Ser. II*, **27**, 246–261, 1974 (in Japanese).

SCHOLZ, C. H., L. R. SYKES, and Y. P. AGGARWAL, Earthquake prediction: A physical basis, *Science*, 803–810, 1973.

SHIONO, K., Focal mechanism of small earthquakes in the Kii peninsula, Kii channel and Shikoku, southwest Japan and some problems related to the plate tectonics, *J. Geosci. Osaka City Univ.*, **16**, 69–91, 1973.

SHIONO, K., Travel time analysis of relatively deep earthquakes in southwest Japan with special reference to the underthrusting to the Philippine Sea plate, *J. Geosci. Osaka City Univ.*, **18**, 37–59, 1974.

SKINNER, B. J., Thermal expansion, in *Handbook of Physical Constants, Geol. Soc. Amer. Mem.*, **97**, 75–96, 1966.

USAMI, T., Descriptive table of major earthquakes in and near Japan which were accompanied by damages, *Bull. Earthq. Res. Inst.*, **44**, 1571–1622, 1966 (in Japanese).